Biochimica et Biophysica Acta 1838 (2014) 842–852

Contents lists available at ScienceDirect

Biochimica et Biophysica Acta

journal homepage: www.elsevier.com/locate/bbamem

Effect of lactose permease presence on the structure and nanomechanics of two-component supported lipid bilayers

Carme Suárez-Germà, Òscar Domènech, M. Teresa Montero, Jordi Hernández-Borrell *

Departament de Fisicoquímica, Facultat de Farmàcia, UB and Institut de Nanociència i Nanotecnologia IN²UB, Barcelona, Catalonia, Spain

ARTICLE INFO

Article history:
Received 1 August 2013
Received in revised form 20 November 2013
Accepted 22 November 2013
Available online 4 December 2013

Keywords:
Lactose permease
Phospholipids
Lateral segregation
AFM
FS

ABSTRACT

In this paper we present a comparative study of supported lipid bilayers (SLBs) and proteolipid sheets (PLSs) obtained from deposition of lactose permease (LacY) of *Escherichia coli* proteoliposomes in plane. Lipid matrices of two components, phosphatidylethanolamine (PE) and phosphatidylglycerol (PG), at a 3:1, mol/mol ratio, were selected to mimic the inner membrane of the bacteria. The aim was to investigate how species of different compactness and stiffness affect the integration, distribution and nanomechanical properties of LacY in mixtures of 1-palmitoyl-2-oleoyl-sn-glycero-3-phosphoethanolamine (POPE) or 1,2-palmitoyl-sn-glycero-3-phosphoethanolamine (DPPE) with 1-palmitoyl-2-oleoyl-sn-glycero-3-[phospho-rac-(1-glycerol)] (POPG). Both compositions displayed phase separation and were investigated by atomic force microscopy (AFM) imaging and force-spectroscopy (FS) mode. PLSs displayed two separated, segregated domains with different features that were characterised by FS and force-volume mode. We correlated the nanomechanical characteristics of solid-like gel phase (L_β) and fluid liquid-crystalline phase (L_α) with phases emerging in presence of LacY. We observed that for both compositions, the extended PLSs showed a L_β apparently formed only by lipids, whilst the second domain was enriched in LacY. The influence of the lipid environment on LacY organisation was studied by performing protein unfolding experiments using the AFM tip. Although the pulling experiments were unspecific, positive events were obtained, indicating the influence of the lipid environment when pulling the protein. A possible influence of the lateral surface pressure on this behaviour is suggested by the higher force required to pull LacY from DPPE:POPG than from POPE:POPG matrices. This is related to higher forces governing protein–lipid interaction in presence of DPPE.

1. Introduction

The cytoplasmic membrane is presently viewed as a heterogeneous system because of the lateral segregation of its fundamental building blocks: lipids and proteins [1]. Depending on the physicochemical properties of its components and the variety of interaction forces that may occur between them, this lateral heterogeneity may have different origins. Lateral segregation has been observed using a wide range of biophysical techniques applied to different model membranes [2] and cells [3]. Lipid domains have also been observed in prokaryotic cells [4], although the size of the nano- and micro-domains remains a matter of controversy [5].

In bilayer model systems, at least two types of lateral phase separation phenomena have been described: those arising from lipid–lipid interactions and those induced by proteins. In this regard, it is a matter of debate whether lipid–lipid interactions govern compartmentalisation of the membrane or whether sustained lipid–protein interactions are responsible for the formation of lipid domains around membrane proteins. A particularly interesting example of lipid–protein aggregation in eukaryotic cells is given by "rafts" [6,7], which are conceived of as dynamic platforms where proteins interact and diffuse along the membrane plane. Another example of protein–phospholipid association is the lateral organisation in highly immobilised annular phospholipids around transmembrane proteins that has been observed using electron spin resonance (ESR) [8]. In fact, whether protein determines phospholipid segregation or vice versa is a subtle reflection of the lipid protein interplay [9].

The use of supported lipid bilayers (SLBs) (membranes supported on a solid substrate) offers several advantages for analysing the topography of samples with nanometre lateral resolution by means of atomic force microscopy (AFM). The insertion of membrane proteins in bilayers can be achieved by reconstitution of proteins in proteoliposomes, which are subsequently spread onto a solid surface (often mica). Thus, by selecting a desired lipid composition that mimics the natural membrane, the protein can interact with the bilayer in a similar way to that occurring in vivo. On the one hand, AFM is one of the most suitable techniques for observing laterally segregated lipid domains [10] and protein self-segregation [11]. On the other hand, local forces arising either from different lipid domains [12] or single proteins embedded in the bilayer [13] can be sensed by using the AFM tip in force spectroscopy (FS) mode. Hence, AFM topography images combined with FS may provide

* Corresponding author.
E-mail address: jordiborrell@ub.edu (J. Hernández-Borrell).

0005-2736/$ – see front matter © 2013 Elsevier B.V. All rights reserved.
http://dx.doi.org/10.1016/j.bbamem.2013.11.015

valuable information not only about protein lateral distribution but also about the influence of the lipid environment on the nanomechanics behind the insertion of membrane proteins in biomimetic systems. It is well-known that the presence of protein within the lipid system is responsible for considerable changes in the organisation and nanomechanics of the entire system [14,15]. In fact, the presence of proteins may promote new lipid–protein domains, as well as extend or modulate the coexistence of phase separation by modifying the transition temperature of the lipid mixtures [16].

The lactose permease (LacY) of *Escherichia coli* (*E. coli*), one of the best studied cytoplasmic membrane proteins, is often taken as a paradigm for the secondary transport proteins that couple the energy stored in an electrochemical ion gradient to a concentration gradient (ß-galactoside/H^+ symport). LacY belongs to what is termed the major facilitator superfamily, most of whose members are predicted to contain 12 transmembrane segments. The secondary structure of LacY consists of 12 transmembrane α-helices, crossing the membrane in a zigzag fashion, which are connected by 11 relatively hydrophilic, periplasmic and cytoplasmic loops, with both amino and carboxyl termini on the cytoplasmic surface [17] (Fig. 1). A three-dimensional (3D) model of a LacY mutant (C154G) [18] and a reaction mechanism derived from X-ray diffraction studies are available [19]. The physiological activity of LacY is influenced by the physicochemical properties of neighbouring phospholipids. LacY is commonly reconstituted in native *E. coli* polar phospholipid membrane extracts as well as in binary mixtures of phosphatidylglycerol (PG) and phosphatidylethanolamine (PE) that mimic the inner membrane of the bacteria [20]. Recent studies have revealed that the activity of LacY is sustained not only by PE but also by phosphatidylcholine (PC) [21]. This study suggests the involvement of both the hydrophilic head group domain and the hydrophobic fatty acid domain of the phospholipids in the activity of LacY.

The objective of the present study was twofold: (i) to investigate how lipid organisation is affected by the incorporation of LacY into binary mixtures of 1-palmitoyl-2-oleoyl-*sn*-glycero-3-[phospho-*rac*-(1-glycerol)] (POPG) and either the heteroacid 1-palmitoyl-2-oleoyl-*sn*-glycero-3-phosphoethanolamine (POPE) or the saturated homoacid 1,2-palmitoyl-*sn*-glycero-3-phosphoethanolamine (DPPE), and (ii) to investigate the changes induced in the protein when modifying the lipid environment. Since both the POPE:POPG and DPPE:POPG (3:1, mol/mol) phospholipid systems display lateral phase separation at the studied temperature [22], it was of interest to determine whether this property influences the integration of the protein. Hence, we first investigated the topography of these SLBs by AFM and determined the nanomechanical properties from the force curves [23]. These experiments were taken as a reference for the topography, FS and force-volume (FV) analyses performed on proteolipids sheets (PLSs) obtained from the extension of proteoliposomes onto the same solid substrate. Thereafter, we conducted unspecific unfolding experiments in order to investigate how LacY is affected by the surrounding phospholipid matrix.

2. Materials and methods

N-Dodecyl-ß-D-maltoside (DDM) was purchased from Anatrace (Maumee, OH, USA). 1-Palmitoyl-2-oleoyl-*sn*-glycero-3-phosphoethanolamine (POPE) and 1-palmitoyl-2-oleoyl-*sn*-glycero-3-[phospho-*rac*-(1-glycerol)] (sodium salt) (POPG) were purchased from Avanti Polar Lipids (Alabaster, AL, USA). Isopropyl-1-thio-ß-D-galactopyranoside (IPTG) was obtained from Sigma Chemical Co. (St. Louis, MO, USA) and polystyrene Bio-Beads® SM-2 were purchased from Bio-Rad (Hercules, CA, USA). All other common chemicals were ACS grade.

2.1. Bacterial strains and protein purification

These procedures have been described in detail in previous papers [24,25]. Briefly, *E. coli* BL21(DE3) cells (Novagen, Madison, WI, USA) transformed with plasmid pCS19 encoding the single-tryptophan mutant W151/C154G LacY provided by Dr. H. Ronald Kaback (UCLA, USA) were grown in Luria–Bertani broth containing ampicillin (100 μg/ml) at 30 °C and induced at the appropriate moment with 0.5 mM IPTG. The cells were disrupted, and the membrane fraction was harvested by ultracentrifugation. The membranes were solubilised by adding DDM and purified by Co (II) affinity chromatography (Talon Superflow, Palo Alto, CA, USA). Protein eluted with 150 mM imidazole was subjected to gel-filtration chromatography using a Superdex 200 10/300 column (GE-Healthcare, Buckinghamshire, UK) equilibrated with 20 mM Tris–HCl (pH 7.6) containing 0.008% DDM. The protein was concentrated using Vivaspin 20 concentrators (30 kDa cut off; Vivascience, Göttingen, Germany) and stored on ice. Protein identification was performed by sodium dodecyl sulphate polyacrylamide gel electrophoresis (SDS-PGE) and protein quantitation was carried out using a Micro BCA kit (Pierce, Rockford, IL).

2.2. Vesicle preparation and protein reconstitution

Liposomes and proteoliposomes were prepared according to previously published methods [22,26]. Briefly, 2:1 (v/v) chloroform/methanol solutions containing appropriate amounts of phospholipids were dried under a stream of oxygen-free N_2 in a conical tube. The total

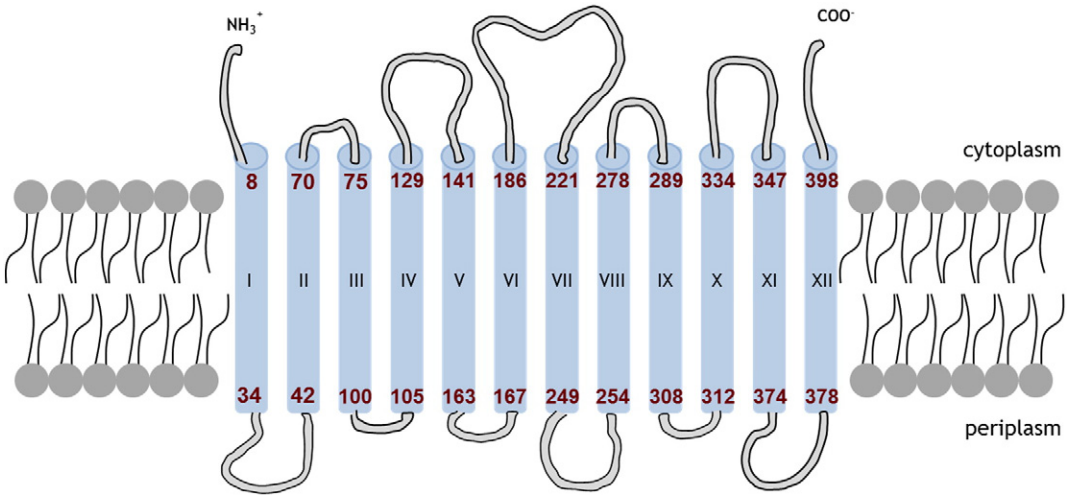

Fig. 1. Secondary structure model of lactose permease showing its topological organisation. Red numbers indicate starting and ending amino acid of each transmembrane α-helix. Protein feature based from PDB 1PV6 entry mapped onto a UniProtKB sequence (www.uniprot.org) [17].

concentration of phospholipids was calculated as a function of the desired lipid-to-protein ratio (LPR) and protein concentration (3.16 μM). The resulting thin film was kept under high vacuum for ~3 h to remove organic solvent traces. Multilamellar liposomes (MLVs) were obtained following redispersion of the film in TRIS buffer (pH 7.60) containing 150 mM NaCl, application of successive cycles of freezing and thawing below and above the phase transition of the phospholipids and sonication for 2 min in a bath sonicator. Large unilamellar vesicles (LUVs) were obtained by extrusion (Mini-extruder, Avanti Polar Lipids, Alabaster, AL) of the MLV trough filters (Whatman Nederland B.V., Netherlands) using a pore size diameter of 100 nm. To obtain proteoliposomes, LUVs supplemented with 0.5% DDM were incubated overnight at room temperature. Solubilised protein was then added to the mixture, and it was incubated at 4 °C for 30 min to obtain a LPR (w/w) of 0.5. Proteoliposomes were obtained after the extraction of DDM using polystyrene beads.

2.3. Supported lipid bilayers and atomic force microscopy

SLBs were spread by vesicle fusion as described elsewhere [22]. Briefly, liposomes or proteoliposomes in TRIS buffer supplemented with 10 mM $CaCl_2$ were deposited onto freshly cleaved mica disks. Samples were incubated at 37 °C for 2 h in an oven, using a water reservoir to prevent evaporation of the water from the sample. Before imaging, samples were washed with non-calcium-supplemented buffer. To perform the experiments, it was necessary to drift equilibrate and thermally stabilise the cantilever in the presence of buffer. Images were acquired at 22 ± 0.5 °C.

Liquid AFM imaging was performed using a Multimode Microscope controlled by Nanoscope V electronics (Bruker, AXS Corporation, Madison, WI). Sample images were acquired in contact mode at scan frequencies of 4–7 Hz using an optimised feedback parameter and applying minimum vertical force. MSNL-10 V-shaped Si_3N_4 cantilevers (Bruker AFM Probes, Camarillo, CA) with a nominal spring constant of 0.03 $N \cdot m^{-1}$ were used. All images were processed using NanoScope Analysis Software (Bruker AXS Corporation, Santa Barbara, CA).

2.4. Force spectroscopy and force-volume measurements

AFM in FS mode was used to obtain nanomechanical magnitudes and to perform protein non-specific unfolding. Individual spring constants of the different cantilevers used were determined using the equipartition theorem. In practical terms the thermal tune calibration was estimated by using the Bruker software provided by the manufacturer. This method gives values which are within the 20% of the values obtained by other methods. Force–distance curves were measured using a constant velocity of 600 $nm \cdot s^{-1}$ between the AFM tip and the sample. When the pulling of the protein was aimed, the force curve was adjusted at low force (0.5–2 nN) pressing the cantilever down for ~1 s. The frequency of the pickups was low in order to avoid possible pick up of two or more proteins simultaneously.

The worm-like chain (WLC) model [27,28], which describes the elastic behaviour of polymer chain elasticity, was used to fit unfolding events found in the force–distance curves, following the expression

$$F(x) = \frac{k_B T}{p}\left[\frac{1}{4}\left(1-\frac{x}{L}\right)^{-2} - \frac{1}{4} + \frac{x}{L}\right] \quad (1)$$

where $F(x)$ is the force at a distance x, k_B is the Boltzmann constant, p is the persistence length (0.4 nm) [29], L is the contour length of the unfolded polypeptide chain and T is the temperature. Force peak events were observed in nearly 10% of all force curves (from a total of ~2000 in each experiment). In order to fit to WLC model only these force curves with well-defined sawtoothlike peaks were accepted. The criterion used to select the unfolding peaks was based in the value of the root mean square error (RMSE), which is a measure of the difference between the values predicted by the WLC model and the values actually observed. Only curves displaying RMSE values < 0.015 nN were accepted.

AFM in FV mode was used to combine the topographical image with FS information. To this end, FV images were recorded at a relative trigger threshold below the breakthrough force of the samples. FV imaging was performed using AFM tips with a nominal spring constant of 0.03 N m^{-1}. Images contained 32 × 32 pixels and were registered with an imaging scan-rate of 1 Hz.

3. Results and discussion

SLBs of POPE:POPG and DPPE:POPG (3:1, mol/mol) are systems that mimic the lipid composition of the inner membrane of *E. coli*. It is well-known that both systems display lateral phase separation at the temperature at which the experiments were conducted [22]. Although it is believed that lipids in natural biomembranes are in fluid liquid-crystalline (L_α) phase, it was considered of interest to investigate the affinity of the protein for the different L_α or solid-like gel (L_β) phases. Therefore, we investigated the topographic and nanomechanical properties of the SLBs of the same composition as that used to reconstitute the protein. AFM topographic images of POPE:POPG (3:1, mol/mol) and DPPE:POPG (3:1 mol/mol) are shown in Figs. 2A and 3A, respectively. The POPE:POPG system showed a fully extended flat bilayer that exhibited the expected coexistence of two lipid phases. We assumed that the higher one was the L_β phase and the lower one, the L_α phase. The step height difference between phases was 0.9 ± 0.1 nm, which matches well with the expected values found elsewhere [30,31]. The absolute height of the L_α phase with respect to the mica could be calculated from some occasional defects found in samples, and was established as 3.8 ± 0.3 nm.

In the DPPE:POPG (3:1, mol/mol) mixture, AFM topographic image in Fig. 3A, a flat featureless bilayer surface with coexistence of L_α and L_β phases was observed. In this case, the height of the L_α domain was established as 5.0 ± 0.2 nm and the height of the L_β domain as 5.7 ± 0.2 nm, both values in concordance with previous results [22].

The nanomechanical study of the bilayers was conducted by analysing the FS curves. Essentially, two magnitudes were extracted by operating in this mode: (i) the breakthrough force or yield threshold force (F_y), i.e. the force that the bilayer can withstand before being indented, and (ii) the adhesion force (F_{adh}), i.e. the pull-off force between the tip and the bilayer [23,32]. Distribution of the F_y and F_{adh} values obtained for POPE:POPG is shown in Fig. 2B and C, respectively. The most probable force values obtained from a Gaussian fitting of the data are shown in Table 1. Concerning F_y (Fig. 2B), L_α and L_β did not show major differences (0.509 ± 0.008 nN for L_α versus 0.464 ± 0.006 nN for L_β), which is reasonably consistent with previous studies [33] and may be attributed to the composition of the buffer used. However, it was not possible to perform a more precise comparison, since earlier experiments were performed at different temperatures and ionic strengths (in this former study, 10 mM of calcium was present), factors which determine the F_y values obtained [34,35]. It could still be hypothesised that the higher values obtained in the present study might be related to the lack of calcium in the medium, which would result in higher electrostatic repulsion between charged phospholipids and the tip, and thus higher forces would need to be overcome for the breakthrough event to occur [33]. For F_{adh} (Fig. 2C), we found similar values for both lipid phases, although L_β showed a slightly higher F_{adh} than L_α (0.292 ± 0.002 nN and 0.205 ± 0.004 nN, respectively). These values are in qualitative agreement with previous studies [36], whilst the quantitative differences were most probably due to variations in ionic strength and temperature. However, the observed trend was the same (L_β F_{adh} > L_α F_{adh}). One possible interpretation for this behaviour would be to relate this to the enhanced stiffening induced by calcium; however, this was not the case in the present study, where the Ca^{2+} concentration was minimised by swabbing it away

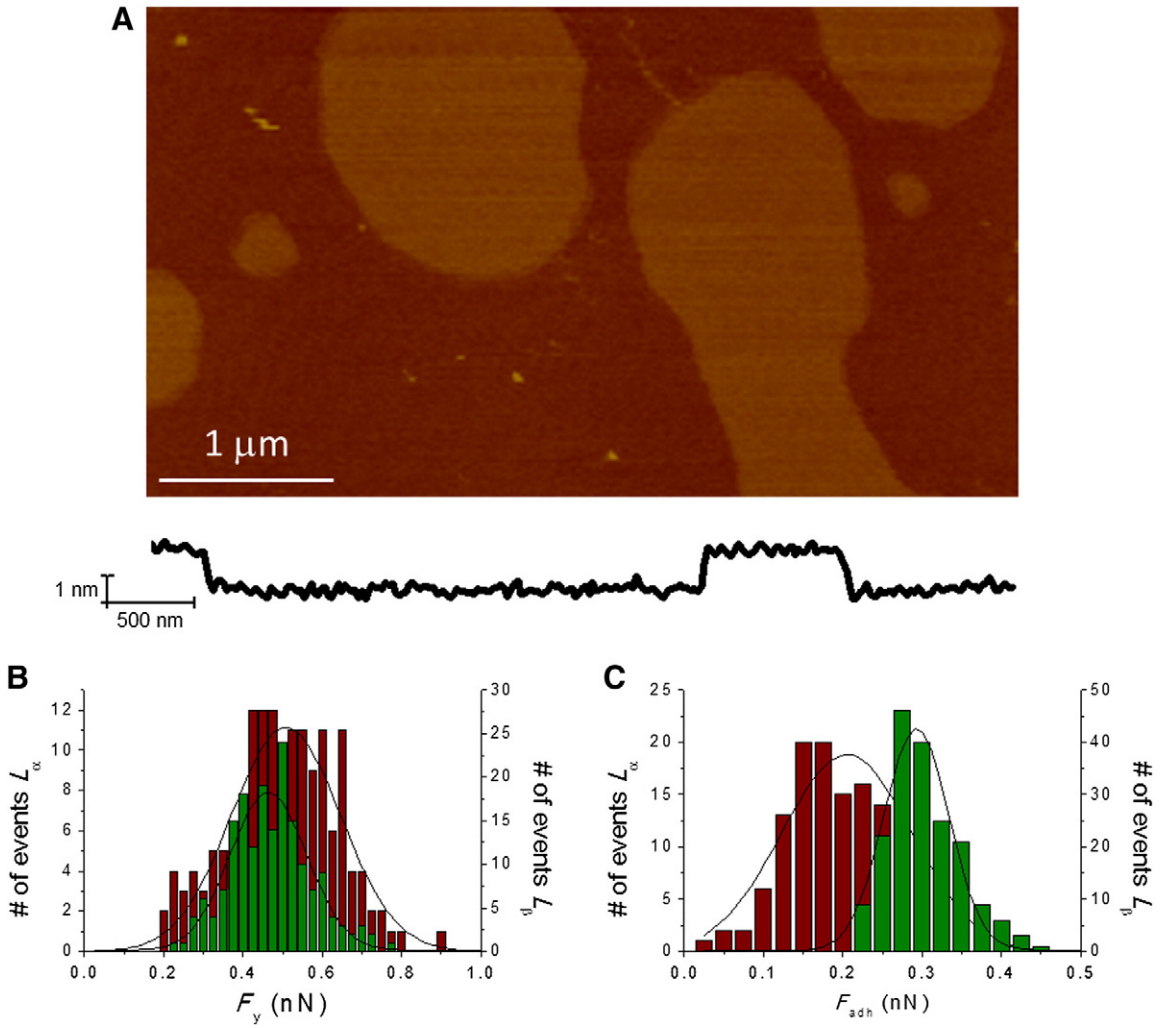

Fig. 2. AFM topographic image and height profile analysis of POPE:POPG (3:1, mol/mol) SLB (Z scale = 10 nm) (A). Histograms present the distribution of forces of L_α phase (red) and L_β phase (green) for F_y (B) and F_{adh} (C). Fittings to a Gaussian distribution are represented in solid lines.

after SLB formation. Therefore, we conclude that adhesion force seems to be sensitive to the presence of Ca^{2+} in the aqueous layer between the SLB and the mica substrate [37,38].

Fig. 3B and C show the distribution of the F_y and F_{adh} values obtained for the DPPE:POPG system. The most probable force values obtained by a Gaussian fitting of the data are shown in Table 1. Concerning F_y, L_α and L_β phases withstood forces of 1.78 ± 0.05 nN and 2.421 ± 0.009 nN, respectively. Note that we required 1.4 times more force to indent the L_β than the L_α domain, which was to be expected, since L_β, enriched in DPPE is the stiffer domain [12]. Also as expected, given the nominal composition, both values were significantly higher than those obtained for the POPE:POPG system. This could be anticipated because of the nature of DPPE, a saturated phospholipid that rigidifies and confers a higher packing to the system [22]. In this regard, DPPE hardens not only L_β phase to a high degree, but also L_α, where it might be present to a lesser extent. We observed that whilst the F_{adh} for the L_α domain in DPPE:POPG was quite similar to the one obtained for L_α in POPE:POPG, the values obtained for the L_β phase were higher. This confirms the trend already described for POPE:POPG in Fig. 2C.

LacY was reconstituted with phospholipids at a LPR ratio (w/w) of 0.5 and the resulting proteoliposomes were then deposited onto mica. Note that this approach yields supported lipid bilayers where LacY is embedded in a random configuration (either facing the substrate or facing the aqueous media) [26]. The LPR used was higher than the one found in most of biological membranes and close to the conditions used for two-dimensional (2D) crystallisation. Notwithstanding the difficulties in obtaining LacY in 2D arrays have been recognized [42] and attributed to the high flexibility of LacY. Since lower LPR values used in previous studies yield isolated and undefined single protein entities [22,31] our strategy in the present work consisted in increasing the LPR ratio close the 2D conditions in order to promote the formation of enriched protein domains. The PLSs obtained by spreading LacY reconstituted in proteoliposomes of POPE:POPG and DPPE:POPG at high LPR values are shown in Figs. 4A and 5A, respectively. In both cases, two laterally segregated domains were observed. As can be seen in Fig. 4A, when LacY was reconstituted in POPE:POPG proteoliposomes there were a lower and a higher domain with step height differences respect to the mica of 5.2 ± 0.2 nm and of 5.6 ± 0.2 nm, respectively. The roughness (*Ra*) values for the lower and higher domain were 0.06 nm and 0.09 nm, respectively. Although the step-height and roughness differences between both domains are small, the measures suggest the existence of two differentiated phases, where the more corrugated domain would correspond to self-segregated proteins.

Fig. 5A shows a proteolipid sheet obtained from deposition of LacY reconstituted in DPPE:POPG proteoliposomes. A bilayer patch can be observed which contained two different domains. The lower one showed a step height with respect to the mica of 4.2 ± 0.2 nm and a *Ra* value of 0.08 nm. The higher one showed a step height of 5.2 ± 0.2 nm and a *Ra* value of 0.15 nm. As can be seen in the inset the higher domain was grainy, which may be likely attributed to the presence of the self-segregated proteins.

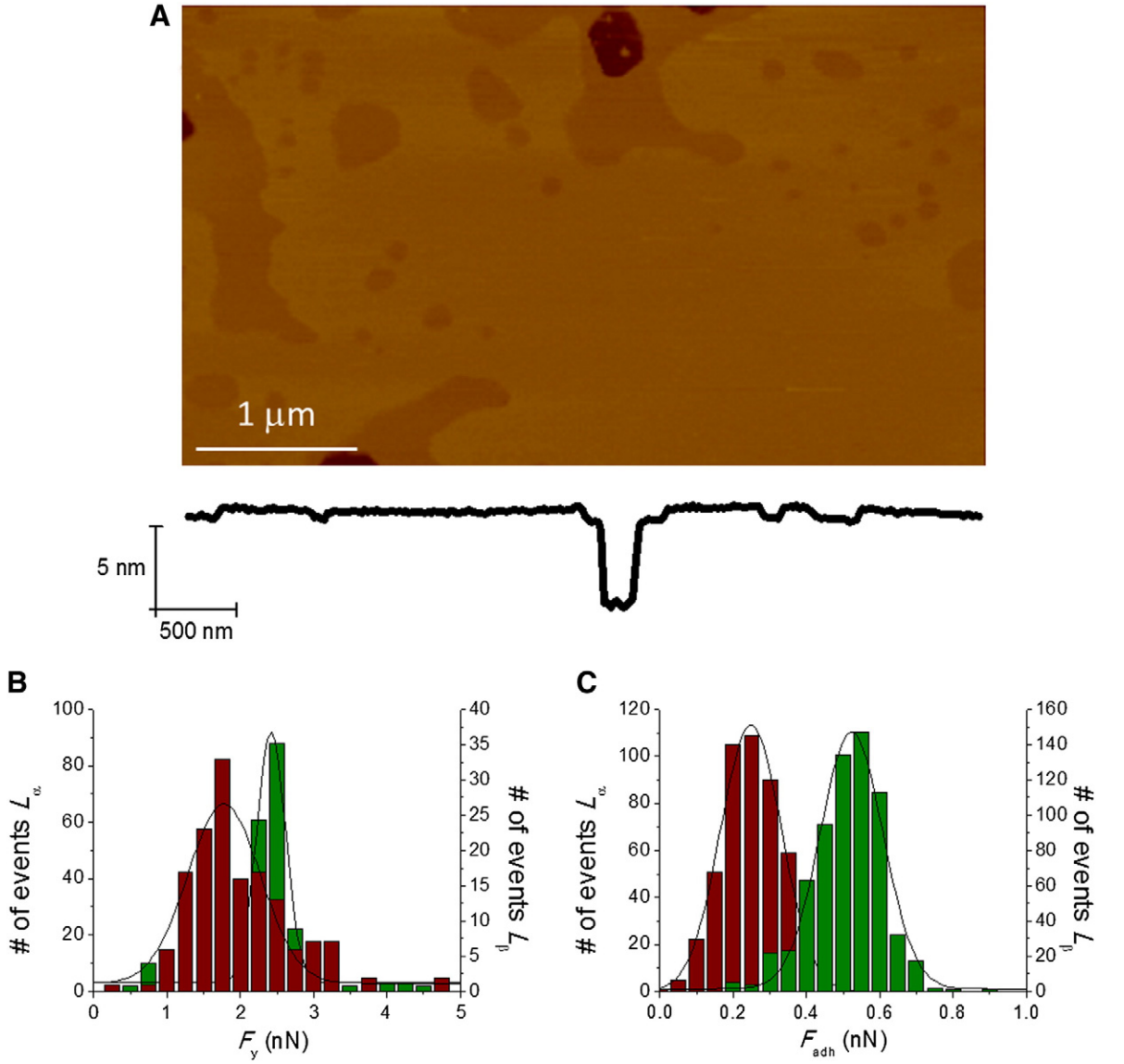

Fig. 3. AFM topographic image and height profile analysis of DPPE:POPG (3:1, mol/mol) SLB (Z scale = 10 nm) (A). Histograms present the distribution of forces of L_α phase (red) and L_β phase (green) for F_y (B) and F_{adh} (C). Fittings to a Gaussian distribution are represented in solid lines.

Conversely to what was observed in a previously published work with lower LPRs [22], it was not possible at higher LPR neither to confirm the existence of L_α and L_β lipid phases nor to identify single isolated entities of the protein. To explain these observations, it is worth to mention that when a transmembrane protein is reconstituted in a binary phospholipid mixture that displays L_α and L_β domains, the protein recruits those phospholipid species which best match its structural requirements and provide the most adequate physicochemical environment [39,40]. Transmembrane proteins are solvated by those phospholipids that reduce the mismatch of the lipid–protein boundary and, as evidenced by ESR, by a lipid annular ring in immediate contact with the protein [41]. Hence, the upper domains absolute height observed in Figs. 4A and 5A may account for the assemblage of LacY, its close phospholipid annular ring and an extra phospholipid nano-domain [39,40]. Therefore, it was considered of interest to conduct a comparative analysis of the domains observed in Figs. 4A and 5A with those observed in Figs. 2A and 3A.

Table 1
Mean F_y and F_{adh} values from data presented in Figs. 2 and 3, fitted to a Gaussian distribution.

		POPE:POPG (3:1, mol:mol)	DPPE:POPG (3:1, mol:mol)
F_y (nN)	L_α	0.509 ± 0.008	1.78 ± 0.05
	L_β	0.464 ± 0.006	2.421 ± 0.009
F_{adh} (nN)	L_α	0.205 ± 0.004	0.249 ± 0.002
	L_β	0.292 ± 0.002	0.523 ± 0.004

To this end, a first approach for understanding the AFM topographic observations in systems with LacY was to compare the step height differences between the SLBs in Figs. 2 and 3 and the lipid and proteolipid domains in Figs. 4 and 5. Thus, when considering the POPE:POPG mixture with LacY (Fig. 4A), we would expect to find a step height difference of 0.9 ± 0.1 nm between L_α and L_β (as shown in Fig. 2A). However, the value between the two domains was 0.4 ± 0.4 nm. It is conceivable that the highest domain would be constituted by close-packed assemblies of LacY protruding above the L_α phase about 1.3 ± 0.5 nm. This measure coincides with the estimated average dimensions of the loops of the protein [18]. This is in concordance with previous AFM observations [22,31]. Consequently, the lower domain would correspond to the L_β phase. Similar rationale can be conducted to analyse the DPPE:POPG mixture in absence and presence of LacY. For this system, the step height differences between both

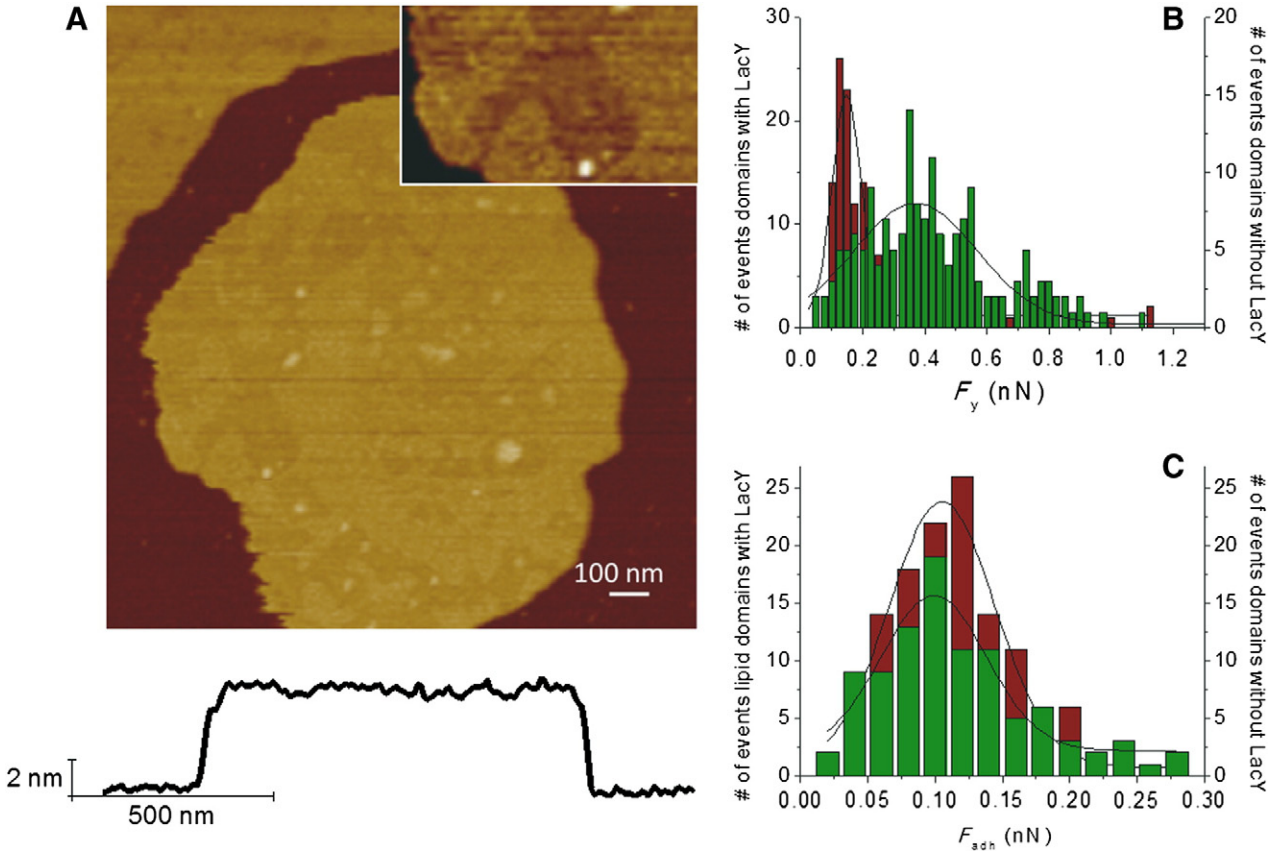

Fig. 4. AFM topographic image and height profile analysis of a SLB composed of POPE:POPG (3:1, mol/mol) with LacY at a LPR (w/w) of 0.5 (Z scale = 15 nm) (A). Insert in A presents a magnified image (470 × 280 nm, Z = 3 nm) where domains with LacY can be distinguished from domains without LacY. Histograms present the distribution of forces of domains with LacY (red) and domains without LacY (green) for F_y (B) and F_{adh} (C). Fittings to a Gaussian distribution are represented in solid lines.

domains were, 0.7 ± 0.4 nm for the SLBs (Fig. 3A) and 1.0 ± 0.4 nm for the PLSs (Fig. 5A). Hence, the height of the self-segregated protein domain can be established in 1.7 ± 0.8 nm, a value that falls within the range of the loops of the protein [18] and previous studies using this same lipid mixture [22]. Other possible interpretations, such as: (i) a protein-free lipid domain corresponding to L_α and a protein-enriched domain corresponding to L_α containing LacY, or (ii) a protein-free lipid domain corresponding to L_α or L_β and a protein-enriched domain corresponding to L_β containing LacY, were discarded because a comparative analysis of step height did not show reliable results. However, it was difficult to go any further with this analysis because the use of detergent in proteoliposomes preparation may significantly change the physicochemical characteristics of the bilayer [11]. For example, it has been reported that for POPE:POPG (3:1, mol/mol) mixtures treated with detergent, height differences between L_α and L_β phases are lower than the height observed before DDM incubation [31]. On the other hand we have demonstrated by measuring energy transfer measurements between the single tryptophan mutant W151/C154G of LacY and pyrene labelled-PE and -PG that there is an enrichment in PE at the annular region of LacY [42,43]. Hence, changes in the composition of the phases may be expected. For this reason, it becomes of interest not only to investigate the distribution of LacY between domains observed in the SLBs but also how the presence of the protein can affect the nanomechanics of the lipid systems.

Nanomechanical information was obtained by extracting force magnitudes from the FS curves applied to the lower and higher domains in PLSs. The distribution of F_y and F_{adh} values was plotted in the histograms shown in Figs. 4B and C and 5B and C for the POPE:POPG and the DPPE:POPG systems, respectively. For a better comparison, the most probable F_y and F_{adh} values corresponding to these compositions are listed in Table 2.

In the case of PLSs obtained from the extension of LacY reconstituted in POPE:POPG, F_y values for the higher and lower domains were 0.124 ± 0.004 nN and 0.37 ± 0.01 nN, respectively. This indicates that domains without protein were less easily punctured than domains containing LacY. Since F_y values in Fig. 2B were similar for L_β and L_α phases, the changes in Fig. 4B indicate that the presence of LacY modified bilayer stiffness. Note, however, that F_y values of the lower domain are in the same range than F_y values of L_β in SLBs. In turn, when analysing F_{adh}, no significant differences were found between domains with and without LacY (0.105 ± 0.003 nN versus 0.1193 ± 0.0014 nN, respectively) (Table 2), which matches reasonably well with the values obtained for protein-free SLBs (Table 1). In general, all F_y and F_{adh} values were lower than the ones presented in Fig. 2B.

In the case of LacY reconstituted in DPPE:POPG, the F_y values followed a similar trend to the one observed when LacY was reconstituted in POPE:POPG. Thus, LacY higher domains showed significantly lower F_y values than lower domains (0.222 ± 0.006 nN and 2.55 ± 0.02 nN, respectively). On the one hand, F_y values in domains without protein compared quite well with F_y values obtained for the L_β domains (Fig. 3B), which is consistent with the hypothesis that this domain may be organised similarly to a L_β phase. On the other hand, domains with LacY showed much lower values than the L_α domains in Fig. 3B, following a similar trend to the one found for POPE:POPG protein-enriched domains. Regarding F_{adh}, both values were similar in presence and absence of LacY (0.212 ± 0.002 nN and 0.237 ± 0.007 nN, respectively), which may be related to the presence of the protein and possible traces of detergent remaining in the system. Again, all values were lower for DPPE:POPG extended proteoliposomes than for DPPE:POPG extended liposomes. The slight differences in the F_y and F_{adh} values could be attributed to changes in the composition of the L_α and L_β phases induced by the selectivity of the protein for PE [25,42], and also to the presence of

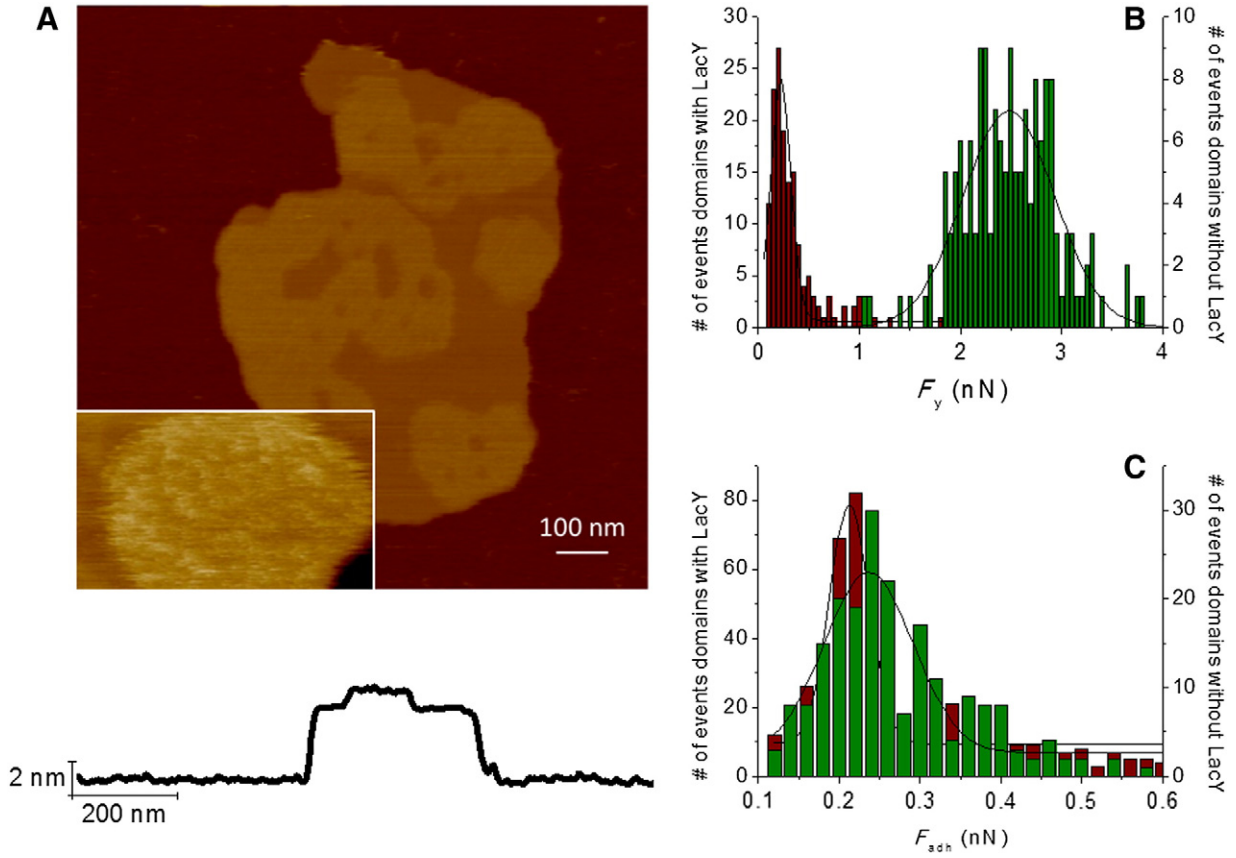

Fig. 5. AFM topographic image and height profile analysis of a SLB composed of DPPE:POPG (3:1, mol/mol) with LacY at a LPR of 0.5 (Z scale = 10 nm) (A). Insert in A presents a magnified image (173 × 104 nm, Z = 3 nm) where domains with LacY can be distinguished from domains without LacY. Histograms present the distribution of forces of domains with LacY (red) and domains without LacY (green) for F_y (B) and F_{adh} (C). Fittings to a Gaussian distribution are represented in solid lines.

some traces of detergent used during the reconstitution of the protein in proteoliposomes [11].

Taking the entire set of F_y values together, we can state that for both lipid mixtures used in LacY reconstitution, the forces obtained in lipid domains with lower roughness, that we assume free of protein were similar to the values obtained for the L_β domains in the lipid SLBs obtained from liposome extension. These results strongly suggest that the lower domains in Figs. 4A and 5A may in fact correspond to L_β phases. Similarly, we may assume that the highest domains may result from the insertion of the protein in the L_α phase and because of the negative curvature tendency of PE [44], the main component of the LacY annular region [43]. In turn, this would lead to greater changes in nanomechanical magnitudes. Thus, F_y values in LacY-enriched domains differ from the same values in protein-free L_α domains. More difficult is a direct interpretation of the F_{adh} values, which can be dramatically affected by other factors, such as area of contact and tip characteristics [45]. Interestingly, we observed that protein–lipid L_α phases from proteoliposomes could be punctured more easily than the L_α phases in the lipid alone. This reinforces the idea that we are actually observing a new fluid phase that includes average bulk properties of protein and its closed solvated phospholipids.

Table 2
Mean F_y and F_{adh} values from data presented in Figs. 4 and 5, fitted to a Gaussian distribution.

		POPE:POPG (3:1, mol:mol)	DPPE:POPG (3:1, mol:mol)
F_y (nN)	With LacY	0.124 ± 0.004	0.222 ± 0.006
	Without LacY	0.370 ± 0.014	2.55 ± 0.02
F_{adh} (nN)	With LacY	0.105 ± 0.003	0.212 ± 0.002
	Without LacY	0.1193 ± 0.0014	0.237 ± 0.007

To elucidate how the presence of proteins affects the lipid bilayer, we investigated the system using the FV [46] mode. Fig. 6A and B show the FV topography images for the two lipid matrices studied, POPE:POPG and DPPE:POPG, respectively. In order to analyse the results, we classified the images into different regions depending on the proximity of each region to the protein-containing domains (see Fig. 6C and D). FV was performed applying low force per pixel, that is, the minimum necessary to avoid bilayer destruction whilst allowing topography recording. Hence, F_{adh} values were notably lower than those obtained from the FS mode due to the fact that tip in FV is not breaking the bilayer and F_{adh} is related to tip penetration [46]. Besides, as reported elsewhere [47,48], the differences in the loading rates between FS and FV result in changes in the viscoelastic properties of the system which may also contribute to the discrepancies in the F_{adh} values obtained from both AFM modes. The F_{adh} values obtained in Fig. 6 increased with the distance from the protein-enriched domain, ranging from 115 ± 16 pN and 10.5 ± 0.8 pN for region 1, to 308 ± 15 pN and 24 ± 2 pN, for the region farthest from the protein, for POPE:POPG and DPPE:POPG, respectively. Indeed, the trend was clear for both lipid matrices: the further from the protein domain, the higher the acquired F_{adh} value. This may be related to two factors: (i) the presence of the protein, which creates a sort of network which stabilises the lipid bilayer; and (ii) the behaviour of the SLBs (Figs. 2C and 3C), where L_β domains presented higher F_{adh} values than L_α domains. This provides support for the coexistence of protein-free L_β phases and LacY-enriched L_α phases. Actually, the F_{adh} values in region 3 of Figs. 6A and 4 in Fig. 6B, may be representative of the boundary region between the L_β and L_α phases.

Having analysed the topographic and nanomechanical changes induced in SLBs when LacY was reconstituted in binary phospholipid systems, we undertook a preliminary investigation of the modifications

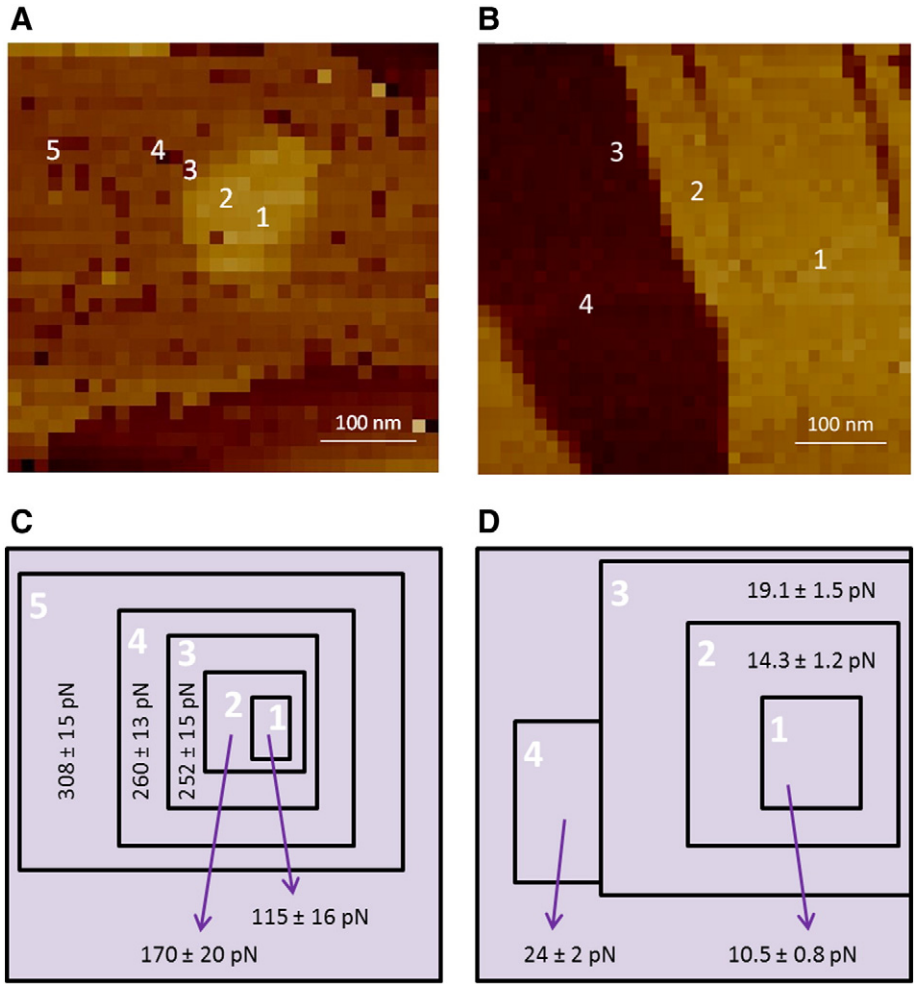

Fig. 6. FV AFM topographic images of POPE:POPG (3:1, mol/mol) with LacY (z scale = 15 nm) (A) and DPPE:POPG (3:1, mol/mol) with LacY (z scale = 10 nm) (B). F_{adh} values obtained from image A (C) and B (D). Regions are numbered indicating proximity to the protein starting from zone 1, closer to LacY.

induced in LacY when embedded in the POPE:POPG and DPPE:POPG matrices. To this end, we performed unspecific FS by approaching the AFM tip close to the PLS domains where self-segregated proteins have been observed (Figs. 4A and 5A). This means that the AFM tip was not chemically functionalised and therefore the protein could be pulled away at any point of its secondary structure. Importantly, we were not pursuing the complete unfolding of the protein in order to unveil its single molecular force spectroscopy spectrum [49] but rather to investigate the stochastic behaviour of the protein embedded in different phospholipid environments. Actually, our objective in these experiments was a semi-quantitative comparison to determine whether force-extension curves of unspecific pulling are modified depending on the composition of the lipid matrix.

In these kinds of experiment, a large number of force curves are obtained, but positive retraction curves account for less than 10% [50]. The large number of unsuccessful events may be attributed to the high

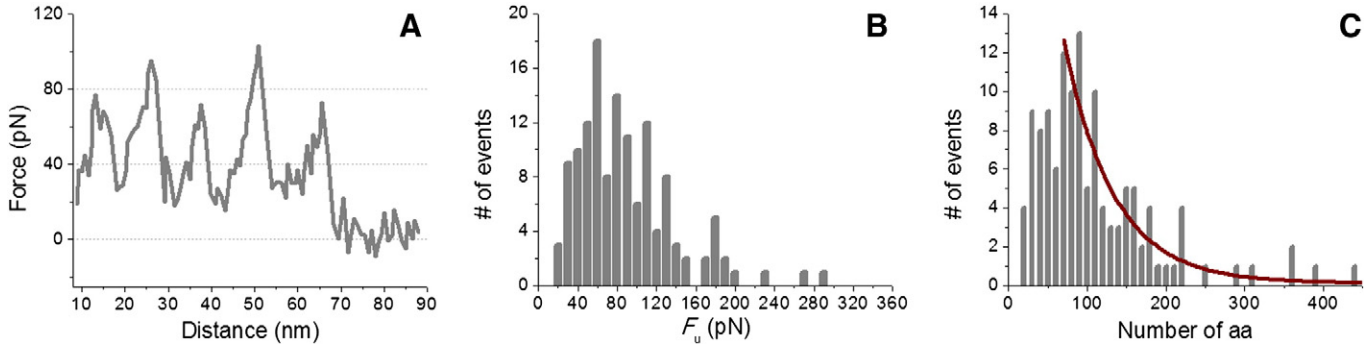

Fig. 7. Representative force–distance curve of single LacY unfolding from POPE:POPG (3:1, mol/mol) matrix (A). Distribution of F_u (B) and distribution of force-curve length (C) are shown for LacY in this lipid matrix. Continuous red line corresponds to an exponential fit to the decay.

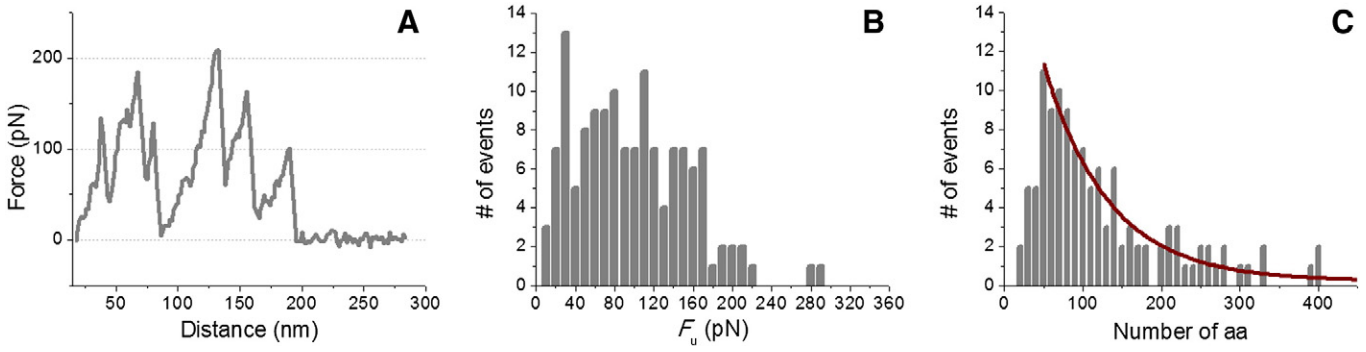

Fig. 8. (A) Representative force–distance curve of single LacY unfolding from DPPE:POPG (3:1, mol/mol) matrix (A). Distribution of F_u (B) and distribution of force-curve length (C) are shown for LacY in this lipid matrix. Continuous red line corresponds to an exponential fit to the decay.

hydrophobicity of the secondary transporters, which are tightly packed in the lipid matrix [51]. Noteworthy, as discussed elsewhere [52] a membrane protein may adapt to lipids or vice versa depending on each particular species. Figs. 7A and 8A show a representative retracting force–distance curve obtained for LacY embedded in POPE:POPG (7A) and in DPPE:POPG (8A) lipid compositions. The retraction curves of LacY displayed characteristic saw-tooth like of force peak features, similar to other secondary transporters characterised by 12 transmembrane α-helix [51,53] with a nonlinear increase in the force on separation that preceded an abrupt return to zero force. It is reasonable to ask if it is possible to pull more than one protein and stretch them simultaneously. But, as can be seen there is some periodicity between the peaks and there are not distinguishable overlapped saw-tooth patterns [54]. Together with our condition of the RMSE test, and considering the observation that dwell times of 1 s greatly increase the probability to obtain these curves, we take this as evidence that we are pulling a single protein entity. For each force–distance curve, several saw-tooth peaks were obtained. By fitting the WLC model to these peaks (Eq. (1)), we determined the force required to unfold a pulled protein segment (unfolding force, F_u) and the approximate number of amino acids that the segment contained.

Although fully extended LacY may present an unfolding curve of about 171.8 nm (427 amino acids considering the His-Tag and 0.4 nm per amino acid residue [29]), the representative retracting force-curve in 7A is shorter, indicating that complete unfolding, as expected for a non-specific pulling and strong lipid–protein interactions, did not occur. Conversely, the representative retracting force-curve in Fig. 8A is closer to a complete unfolding of the protein. Indeed, the total lengths of the unfolding curves were highly variable depending on the tip-protein contact point and whether the protein was completely unfolded or not. For this reason, entire unfolding curves could not be overlaid and averaged in this study.

Figs. 7B and 8B show the distribution of the F_u values obtained from pulling LacY embedded in POPE:POPG and DPPE:POPG matrices, respectively. As can be seen, the main F_u values were centred in different regions depending on the phospholipid binary system used in reconstitution. The presence of a single peak in both histograms may be indicative of a monomeric protein organisation [55]. The average unfolding rupture forces corresponding to LacY embedded in POPE:POPG and DPPE:POPG were 72.7 ± 3.6 pN and 91.4 ± 4.3 pN, respectively. These values are in agreement with the unfolding from 2 to 6 α-helices (see Fig. 1), since it is accepted that the force required unfolding a primarily α-helical segment should range between 15 and 25 pN [55,56]. These findings would appear to indicate that higher force is required to unfold LacY from the DPPE:POPG matrix than from the POPE:POPG matrix. These observations suggest that the forces governing the protein–lipid interaction when DPPE is the predominant lipid are slightly more important than when the main lipid is POPE and thus LacY might be more tightly inserted in this system. That can be related to two former observations: (i) PE has been described as a chaperone for LacY and, at the same time it is thought to be essential for LacY physiological activity [42,57,58]; and (ii) the acyl chain curvature plays a defined role in the adaptation to the surface of the protein [24]. Both observations are in agreement with the fact that flexible proteins like LacY adapt better to more rigid phospholipids as it is the case of DPPE [1,52]. Additionally, this coincides with recent finding of Bogdanov's group that demonstrates the relevance of the acyl chains in the LacY activity [21]. Of course, it is tempting to relate this behaviour to the different lateral pressures [16] exerted by each phospholipid. As we have previously shown from interfacial phospholipid monolayers, DPPE presents a larger compressibility modulus than POPE [22,59].

Further investigation into the pulling events yielded an estimation of the number of amino acids extracted in each unfolding event. The distributions corresponding to the POPE:POPG and DPPE:POPG matrices are shown in Figs. 7C and 8C, respectively. As can be seen, the most probable values obtained by retrieving the tip from the protein-enriched domains observed in the POPE:POPG and DPPE:POPG matrices were 76 ± 3 and 77 ± 4 amino acids, respectively. This would correspond, on average, to a most probable unfolding in a row of 2.3 α-helices for both lipid mixtures (on average, LacY presents 33.2 amino acids per α-helix and contiguous loop, Fig. 1). Interestingly, although DPPE:POPG presented the highest F_u value, it showed the same number of amino acids per pulling event as that obtained from retrieving the tip from POPE:POPG. This may indicate that the required force per amino acid in DPPE:POPG is higher than that required in the POPE:POPG composition, reinforcing the hypothesis that the lateral pressure [16] exerted by the phospholipids is a relevant parameter to take into account. This is important, because pulling experiment outputs of transmembrane protein may vary depending on the lipid matrix used for reconstitution. Lastly, the probability of total unfolding of LacY increased the more α-helices (and consequently amino acids) were pulled. Hence, the unfolding length histograms respond to a decrease in the # of events as length increases, which can be seen by the exponential decay fitting performed in Figs. 7C and 8C. A similar behaviour was found for other systems [60].

Taken together, the results presented in this paper demonstrate that the presence of a protein greatly modifies lateral phase segregation in lipid systems. Clearly, when LacY is incorporated into the lipid matrices, two phases are present, but different of the pure L_β or L_α phases. However, a comparative height analysis and the nanomechanical analysis performed on each domain strongly suggest that the domain where the protein is not apparent corresponded to a L_β lipid domain, whilst the domain enriched in LacY corresponded to a new domain where the characteristics of the pure L_α phase had been slightly modified. There is a preferential insertion of LacY for these like-fluid domains mainly composed of POPG. Note, however, that this is not in contradiction with the presence of POPE or DPPE (to a lesser extent) at the boundary or annular region of LacY.

This finding is in agreement with previous studies based on FRET measurements. Furthermore, the unspecific unfolding approach employed here, which was not aimed at structural elucidation of the protein, showed a differential behaviour depending on the PE acyl chain composition. These results indicate the important influence of the lateral pressure achieved at core levels, as suggested by molecular dynamic simulations.

Acknowledgements

C. S. G. is the recipient of a FPI fellowship from the Spanish Ministerio de Economía y Competitividad of Spain. This study was supported by grant CTQ-2008-03922/BQU from the Spanish Ministerio de Ciencia e Innovación of Spain. The authors also thank the Universitat de Barcelona for financial support and Laura Picas for valuable insights and comments.

References

[1] D.M. Engelman, Membranes are more mosaic than fluid, Nature 438 (2005) 578–580.
[2] M.C. Giocondi, D. Yamamoto, E. Lesniewska, P.E. Milhiet, T. Ando, C. Le Grimellec, Surface topography of membrane domains, Biochim. Biophys. Acta 1798 (2010) 703–718.
[3] D. Lingwood, K. Simons, Lipid rafts as a membrane-organizing principle, Science 327 (2010) 46–50.
[4] E. Mileykovskaya, W. Dowhan, Visualization of phospholipid domains in *Escherichia coli* by using the cardiolipin-specific fluorescent dye 10-*N*-nonyl acridine orange, J. Bacteriol. 182 (2000) 1172–1175.
[5] L.M.S. Loura, R.F.M. de Almeida, L.C. Silva, M. Prieto, FRET analysis of domain formation and properties in complex membrane systems, Biochim. Biophys. Acta 1788 (2009) 209–224.
[6] D.A. Brown, E. London, Functions of lipid rafts in biological membranes, Annu. Rev. Cell Dev. Biol. 14 (1998) 111–136.
[7] A. Rietveld, K. Simons, The differential miscibility of lipids as the basis for the formation of functional membrane rafts, Biochim. Biophys. Acta 1376 (1998) 467–479.
[8] A.G. Lee, How lipids affect the activities of integral membrane proteins, Biochim. Biophys. Acta 1666 (2004) 62–87.
[9] J.A. Poveda, A.M. Fernández, J.A. Encinar, J.M. González-Ros, Protein-promoted membrane domains, Biochim. Biophys. Acta 1778 (2008) 1583–1590.
[10] P.F. Almeida, W.L. Vaz, T.E. Thompson, Lateral diffusion and percolation in two-phase, two-component lipid bilayers. Topology of the solid-phase domains in-plane and across the lipid bilayer, Biochemistry 31 (1992) 7198–7210.
[11] A. Berquand, D. Lévy, F. Gubellini, C. Le Grimellec, P.E. Milhiet, Influence of calcium on direct incorporation of membrane proteins into in-plane lipid bilayer, Ultramicroscopy 107 (2007) 928–933.
[12] S. Garcia-Manyes, L. Redondo-Morata, G. Oncins, F. Sanz, Nanomechanics of lipid bilayers: heads or tails? J. Am. Chem. Soc. 132 (2010) 12874–12886.
[13] D. Fotiadis, S. Scheuring, S.A. Müller, A. Engel, D.J. Müller, Imaging and manipulation of biological structures with the AFM, Micron 33 (2002) 385–397.
[14] P.J. Quinn, A lipid matrix model of membrane raft structure, Prog. Lipid Res. 49 (2010) 390–406.
[15] G. van den Bogaart, K. Meyenberg, H.J. Risselada, H. Amin, K.I. Willig, B.E. Hubrich, M. Dier, S.W. Hell, H. Grubmüller, U. Diederichsen, R. Jahn, Membrane protein sequestering by ionic protein–lipid interactions, Nature 479 (2011) 552–555.
[16] D. Marsh, Protein modulation of lipids, and vice-versa, in membranes, Biochim. Biophys. Acta 1778 (2008) 1545–1575.
[17] T.U. Consortium, Update on activities at the Universal Protein Resource (UniProt) in 2013, Nucleic Acids Res. 41 (2013) D43–D47.
[18] J. Abramson, I. Smirnova, V. Kasho, G. Verner, H.R. Kaback, S. Iwata, Structure and mechanism of the lactose permease of *Escherichia coli*, Science 301 (2003) 610–615.
[19] L. Guan, H.R. Kaback, Lessons from lactose permease, Annu. Rev. Biophys. Biomol. Struct. 35 (2006) 67–91.
[20] P. Van Gelder, F. Dumas, M. Winterhalter, Understanding the function of bacterial outer membrane channels by reconstitution into black lipid membranes, Biophys. Chem. 85 (2000) 153–167.
[21] H. Vitrac, M. Bogdanov, W. Dowhan, Proper fatty acid composition rather than an ionizable lipid amine is required for full transport function of lactose permease from *Escherichia coli*, J. Biol. Chem. 288 (2013) 5873–5885.
[22] C. Suárez-Germà, M.T. Montero, J. Ignés-Mullol, J. Hernández-Borrell, Ò. Domènech, Acyl chain differences in phosphatidylethanolamine determine domain formation and LacY distribution in biomimetic model membranes, J. Phys. Chem. B 115 (2011) 12778–12784.
[23] L. Picas, P.E. Milhiet, J. Hernández-Borrell, Atomic force microscopy: a versatile tool to probe the physical and chemical properties of supported membranes at the nanoscale, Chem. Phys. Lipids 165 (2012) 845–860.
[24] C. Suárez-Germà, L.M.S. Loura, M. Prieto, Ò. Domènech, J.M. Campanera, M.T. Montero, J. Hernández-Borrell, Phospholipid–lactose permease interaction as reported by a head-labeled pyrene phosphatidylethanolamine: a FRET study, J. Phys. Chem. B 117 (2013) 6741–6748.
[25] C. Suárez-Germà, L.M.S. Loura, M. Prieto, Ò. Domènech, M.T. Montero, A. Rodríguez-Banqueri, J.L. Vázquez-Ibar, J. Hernández-Borrell, Membrane protein–lipid selectivity: enhancing sensitivity for modeling FRET data, J. Phys. Chem. B 116 (2012) 2438–2445.
[26] S. Merino-Montero, Ò. Domènech, M.T. Montero, J. Hernández-Borrell, Preliminary atomic force microscopy study of two-dimensional crystals of lactose permease from *Escherichia coli*, Biophys. Chem. 119 (2006) 78–83.
[27] C. Bustamante, J. Marko, E. Siggia, S. Smith, Entropic elasticity of lambda-phage DNA, Science 265 (1994) 1599–1600.
[28] A. Janshoff, M. Neitzert, Y. Oberdörfer, H. Fuchs, Force spectroscopy of molecular systems-single molecule spectroscopy of polymers and biomolecules, Angew. Chem. Int. Ed. Engl. 39 (2000) 3212–3237.
[29] S.R.K. Ainavarapu, J. Brujic, H.H. Huang, A.P. Wiita, H. Lu, L. Li, K.A. Walther, M. Carrion-Vazquez, H. Li, J.M. Fernandez, Contour length and refolding rate of a small protein controlled by engineered disulfide bonds, Biophys. J. 92 (2007) 225–233.
[30] M. Giocondi, V. Vié, E. Lesniewska, P.E. Milhiet, M. Zinke-Allmang, C. Le Grimellec, Phase topology and growth of single domains in lipid bilayers, Langmuir 17 (2001) 1653–1659.
[31] L. Picas, A. Carretero-Genevrier, M.T. Montero, J.L. Vázquez-Ibar, B. Seantier, P.E. Milhiet, J. Hernández-Borrell, Preferential insertion of lactose permease in phospholipid domains: AFM observations, Biochim. Biophys. Acta 1798 (2010) 1014–1019.
[32] Y. Dufrêne, W. Barger, J. Green, G. Lee, Nanometer-scale surface properties of mixed phospholipid monolayers and bilayers, Langmuir 7463 (1997) 4779–4784.
[33] L. Picas, M.T. Montero, A. Morros, M.E. Cabañas, B. Seantier, P.E. Milhiet, J. Hernández-Borrell, Calcium-induced formation of subdomains in phosphatidylethanolamine–phosphatidylglycerol bilayers: a combined DSC, ^{31}P NMR, and AFM study, J. Phys. Chem. B 113 (2009) 4648–4655.
[34] A. Alessandrini, H.M. Seeger, A. Di Cerbo, T. Caramaschi, P. Facci, What do we really measure in AFM punch-through experiments on supported lipid bilayers? Soft Matter 7 (2011) 7054–7064.
[35] S. Garcia-Manyes, G. Oncins, F. Sanz, Effect of ion-binding and chemical phospholipid structure on the nanomechanics of lipid bilayers studied by force spectroscopy, Biophys. J. 89 (2005) 1812–1826.
[36] R.M.A. Sullan, J.K. Li, S. Zou, Direct correlation of structures and nanomechanical properties of multicomponent lipid bilayers, Langmuir 25 (2009) 7471–7477.
[37] E. Sackmann, Supported membranes: scientific and practical applications, Science 271 (1996) 43–48.
[38] P.E. Milhiet, F. Gubellini, A. Berquand, P. Dosset, J.L. Rigaud, C. Le Grimellec, D. Lévy, High-resolution AFM of membrane proteins directly incorporated at high density in planar lipid bilayer, Biophys. J. 91 (2006) 3268–3275.
[39] L. Picas, M.T. Montero, A. Morros, J.L. Vázquez-Ibar, J. Hernández-Borrell, Evidence of phosphatidylethanolamine and phosphatidylglycerol presence at the annular region of lactose permease of *Escherichia coli*, Biochim. Biophys. Acta 1798 (2009) 291–296.
[40] M. Bogdanov, J. Xie, P. Heacock, W. Dowhan, To flip or not to flip: lipid–protein charge interactions are a determinant of final membrane protein topology, J. Cell Biol. 182 (2008) 925–935.
[41] F.I. Valiyaveetil, Y. Zhou, R. MacKinnon, Lipids in the structure, folding, and function of the KcsA K^+ channel, Biochemistry 41 (2002) 10771–10777.
[42] L. Picas, C. Suárez-Germà, M.T. Montero, J.L. Vázquez-Ibar, J. Hernández-Borrell, M. Prieto, L.M.S. Loura, Lactose permease lipid selectivity using Förster resonance energy transfer, Biochim. Biophys. Acta 1798 (2010) 1707–1713.
[43] C. Suárez-Germà, L.M.S. Loura, Ò. Domènech, M.T. Montero, J.L. Vázquez-Ibar, J. Hernández-Borrell, Phosphatidylethanolamine–lactose permease interaction: a comparative study based on FRET, J. Phys. Chem. B 116 (2012) 14023–14028.
[44] F. Dumas, J.F. Tocanne, G. Leblanc, M.C. Lebrun, Consequences of hydrophobic mismatch between lipids and melibiose permease on melibiose transport, Biochemistry 39 (2000) 4846–4854.
[45] J. Israelachvili, Electrostatic Forces Between Surfaces in Liquid, in: Intermolecular and Surface Forces, 3rd ed. Academic Press, San Diego, 2011. 291–340.
[46] H. An, M.R. Nussio, M.G. Huson, N.H. Voelcker, J.G. Shapter, Material properties of lipid microdomains: force-volume imaging study of the effect of cholesterol on lipid microdomain rigidity, Biophys. J. 99 (2010) 834–844.
[47] I.D. Medalsy, D.J. Müller, Nanomechanical properties of proteins and membranes depend on loading rate and electrostatic interactions, ACS Nano 7 (2013) 2642–2650.
[48] A. Alessandrini, H.M. Seeger, T. Caramaschi, P. Facci, Dynamic force spectroscopy on supported lipid bilayers: effect of temperature and sample preparation, Biophys. J. 103 (2012) 38–47.
[49] D. Muller, AFM: a nanotool in membrane biology, Biochemistry 47 (2008) 7986–7998.
[50] K.T. Sapra, H. Besir, D. Oesterhelt, D.J. Muller, Characterizing molecular interactions in different bacteriorhodopsin assemblies by single-molecule force spectroscopy, J. Mol. Biol. 340 (2004) 1143–1152.
[51] A. Kedrov, C. Ziegler, H. Janovjak, W. Kühlbrandt, D.J. Müller, Controlled unfolding and refolding of a single sodium-proton antiporter using atomic force microscopy, J. Mol. Biol. 340 (2004) 1143–1152.
[52] I. Medalsy, U. Hensen, D.J. Muller, Imaging and quantifying chemical and physical properties of native proteins at molecular resolution by force-volume AFM, Angew. Chem. Int. Ed. Engl. 50 (2011) 12103–12108.
[53] A. Kedrov, M. Krieg, C. Ziegler, W. Kuhlbrandt, D.J. Muller, Locating ligand binding and activation of a single antiporter, EMBO Rep. 6 (2005) 668–674.
[54] A.F. Oberhauser, P.K. Hansma, M. Carrion-Vazquez, J.M. Fernandez, Stepwise unfolding of titin under force-clamp atomic force microscopy, Proc. Natl. Acad. Sci. U. S. A. 98 (2001) 468–472.
[55] L.N. Rahman, F. McKay, M. Giuliani, A. Quirk, B.A. Moffatt, G. Harauz, J.R. Dutcher, Interactions of *Thellungiella salsuginea* dehydrins TsDHN-1 and TsDHN-2 with membranes at cold and ambient temperatures-Surface morphology and single-molecule force measurements show phase separation, and reveal tertiary and quaternary associations, Biochim. Biophys. Acta 1828 (2013) 967–980.

[56] M. Rief, J. Pascual, M. Saraste, H.E. Gaub, Single molecule force spectroscopy of spectrin repeats: low unfolding forces in helix bundles, J. Mol. Biol. 286 (1999) 553–561.
[57] C.C. Chen, T.H. Wilson, The phospholipid requirement for activity of the lactose carrier of *Escherichia coli*, J. Biol. Chem. 259 (1984) 10150–10158.
[58] W. Dowhan, M. Bogdanov, Lipid-dependent membrane protein topogenesis, Annu. Rev. Biochem. 78 (2009) 515–540.
[59] L. Picas, C. Suárez-Germà, M.T. Montero, Ò. Domènech, J. Hernández-Borrell, Miscibility behavior and nanostructure of monolayers of the main phospholipids of *Escherichia coli* inner membrane, Langmuir 28 (2011) 701–706.
[60] L.N. Liu, K. Duquesne, F. Oesterhelt, J.N. Sturgis, S. Scheuring, Forces guiding assembly of light-harvesting complex 2 in native membranes, Proc. Natl. Acad. Sci. U. S. A. 108 (2011) 9455–9459.